AD-A172 585 MINIMIZING THE REFLECTION OF ELECTROMAGNETIC WAVES BY SURFACE IMPEDANCE(U) WISCONSIN UNIV-MADISON MATHEMATICS RESEARCH CENTER T J BRIDGES ET AL. JUL 86 MRC-TSR-2942 1/1

UNCLASSIFIED DAAG29-80-C-0041 F/G 20/14 NL

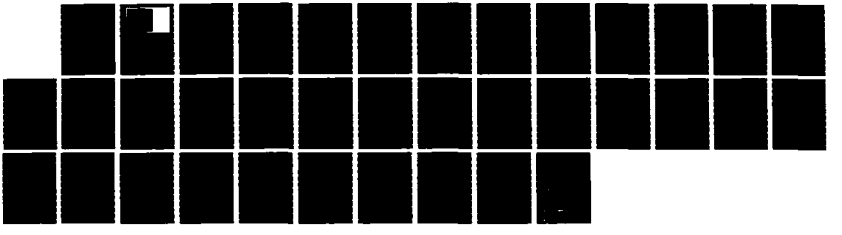

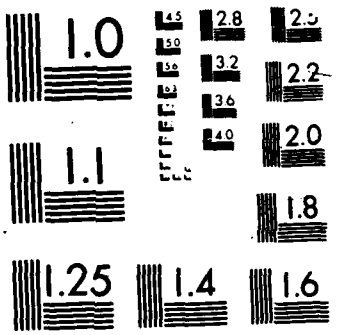
1.0
1.1
1.25
1.4
1.6
1.8
2.0
2.2
2.8
3.2
3.6
4.0

MRC Technical Summary Report #2942

MINIMIZING THE REFLECTION OF ELECTROMAGNETIC WAVES BY SURFACE IMPEDANCE

T. J. Bridges, G. Chen and G. Crosta

Mathematics Research Center
University of Wisconsin—Madison
610 Walnut Street
Madison, Wisconsin 53705

July 1986

(Received June 20, 1986)

Approved for public release
Distribution unlimited

Sponsored by

U. S. Army Research Office
P. O. Box 12211
Research Triangle Park
North Carolina 27709

National Science Foundation
Washington, DC 20550

UNIVERSITY OF WISCONSIN-MADISON
MATHEMATICS RESEARCH CENTER

MINIMIZING THE REFLECTION OF ELECTROMAGNETIC WAVES BY SURFACE IMPEDANCE

T. J. Bridges[1,*], G. Chen[2,**] and G. Crosta[3,***]

Technical Summary Report #2942
July 1986

ABSTRACT

In an empty halfspace a point source emits electromagnetic waves of fixed frequency and arbitrary polarization. The fields reflected by an imperfectly conducting plane, characterized by a constant, isotropic surface impedance, are determined by means of the geometrical optics approximation. An optimization method is used to compute the surface impedance, which minimizes a given function of the e.m. fields (e.g. the average energy density) at a given observation point. The properties of the functions to be minimized are studied and a set of numerical results is presented and discussed.

AMS (MOS) Subject Classifications: 35L05, 49E05, 78A50

Key Words: electromagnetic waves, geometrical optics, control theory, minimizing reflection

Work Unit Number 2 (Physical Mathematics)

---

[1]Mathematics Research Center, University of Wisconsin-Madison, Madison, WI 53705.

[2]Department of Mathematics and Operations Research, Pennsylvania State University, University Park, PA 16802.

[3]Dip. di Scienze dell' Informazione, Università di Milano, via Moretto da B. 9, I-20133 Milano, ITALY.

---

[*]Sponsored by the United States Army under Contract No. DAAG29-80-C-0041. This material is based upon work supported by the National Science Foundation under Grant No. DMS-8210950, Mod. 4.

[**]Supported in part by National Science Foundation Grant Nos. MCS78-22830 and DMS84-01297.

[***]Supported by ICES research project, MPI 40%, 1983, 1984, 1985.

MINIMIZING THE REFLECTION OF ELECTROMAGNETIC WAVES BY SURFACE IMPEDANCE

T. J. Bridges[1,*], G. Chen[2,**] and G. Crosta[3,***]

I. INTRODUCTION

I.1. Problem statement

We consider an optimization problem related to the reflection of electromagnetic waves. A point source of monochromatic waves, characterized by a dipole vector, is located in an empty halfspace and illuminates an unbounded plane surface, having constant surface impedance. If the latter satisfies some properties to be defined below, the incoming wave energy is partly absorbed and partly reflected. By means of the geometrical optics approximation the reflected fields are evaluated. Since they are functions of position as well as other parameters, we state the following problems:

a) given an observation point in the halfspace, which need not coincide with the source, determine e.g. how the e.m. energy density, or the real part of the modulus of the Poynting vector at that point, depend on the surface impedance as its real and imaginary part are varied (direct problem);

[1]Mathematics Research Center, University of Wisconsin-Madison, Madison, WI 53705.

[2]Department of Mathematics and Operations Research, Pennsylvania State University, University Park, PA 16802.

[3]Dip. di Scienze dell' Informazione, Università di Milano, via Moretto da B. 9, I-20133 Milano, ITALY.

*Sponsored by the United States Army under Contract No. DAAG29-80-C-0041. This material is based upon work supported by the National Science Foundation under Grant No. DMS-8210950, Mod. 4.

**Supported in part by National Science Foundation Grant Nos. MCS78-22830 and DMS84-01297.

***Supported by ICES research project, MPI 40%, 1983, 1984, 1985.

b) given an observation point as above, find the value of the surface impedance within a prescribed set which minimizes either of the above mentioned field functions (minimization problem);

c) after finding the optimal impedance value as of problem b), determine how either of the above field functions depends on position as the observation point is moved (position sensitivity problem).

Problem a) consists of making the reflecting plane almost "invisible" to a particular observer. This study is our first approach towards the widely publicized "stealth" problem, which aims at minimizing the radar cross section of some obstacles. The model we adopt is simplified, however, with respect to any practical situation: nevertheless we believe our methods and results are helpful in outlining some features of the general problem.

In the following we introduce the background material. In Section II we calculate the first two terms in the geometrical optics expansion of the reflected magnetic and electric fields. In Section III we state the optimization problems for some objective functions, which depend on the complex surface impedance through the reflected fields. Minimization of said functions is carried out by a steepest descent method, incorporated into a recently developed computer code. Several results are shown and discussed.

I.2. The impedance boundary condition

Let D be a halfspace; $\mathbf{x} = (x_1, x_2, x_3)$, where $x_3 > d$, denotes a point in D and ∂D the $x_3 = d$ plane. Then $\bar{D}$ will stand for $D \cup \partial D$. The electromagnetic fields $(\mathbf{H}, \mathbf{E})$ considered herewith are complex quantities having a suppressed time dependence $\exp(-i\omega t)$. Both $\mathbf{H}$ and $\mathbf{E}$ satisfy homogeneous Maxwell's equations everywhere in D, except at $\mathbf{x}_s$, where the source of a monochromatic spherical wave is located (see Section I.5). We assume that the $x_3 = d$ plane is an imperfect conductor. In order to account for the nonzero resistance of the latter and for the related inductive effects, the following impedance boundary condition is specified:

$$-\hat{n} \times E = Z(\hat{n} \times \hat{n} \times H), \quad \text{at } \partial D \tag{1.1}$$

where $\hat{n}$ is the outward unit normal vector and Z is a complex valued 3×3 matrix, named the surface impedance. In the most general case its entries may depend on $x \in \partial D$. It can be shown (Jones [1], pp. 511 ff) that, if:

$$Z + Z^* > 0 , \tag{1.2}$$

where Z^* is the hermitian conjugate of Z, i.e. if $Z + Z^*$ is positive definite, then (1.1) plus some adequate radiation conditions are sufficient for Maxwell's equations to have a unique solution in $\bar{D}$.

If Z is replaced by the complex scalar $z := \rho + i\tau$, (1.2) becomes:

$$\rho = \mathrm{Re}\ z > 0 , \tag{1.3}$$

which is easily seen to yield a power dissipative boundary condition.

Before considering our problems in detail, we must comment on (1.1). It can e.g. be obtained under the hypothesis that fields penetrating from the surface into the material fall off as (Collin [2], pp. 16-17) e.g.:

$$E(x) = E(x_1, x_2, d) \exp[-(d - x_3)/\delta_s], \quad x_3 \leq d \tag{1.4}$$

where δ_s, the "skin depth", is related to conductivity σ, angular frequency ω and vacuum magnetic permeability μ_0 by:

$$\delta_s := \sqrt{2/\omega\mu_0\sigma} . \tag{1.5}$$

If the material is isotropic, it can be shown that the corresponding surface impedance reads:

$$z = (1 + i)/\sigma\delta_s . \tag{1.6}$$

Moreover, for (1.5) to hold it is required that:

$$\delta_s \ll \lambda = \frac{2\pi}{\omega\sqrt{\mu_0\varepsilon_0}} . \tag{1.7}$$

(1.6) and (1.7) respectively shall be used as a physical realizability constraint in the minimization problem and as an "a posteriori" inequality for the validity range of our model.

I.3. The geometrical optics solution method

According to geometrical optics and diffraction theory (Luneburg [3], Keller [4], Klein and Kay [5]) the asymptotic solution to a diffraction problem may be expressed as the sum of the incident and the scattered fields:

$$(\mathbf{H},\mathbf{E}) = (\mathbf{H}^I,\mathbf{E}^I) + (\mathbf{H}^S,\mathbf{E}^S) \ , \tag{1.8}$$

where the scattered field $(\mathbf{H}^S,\mathbf{E}^S)$ is further decomposed into the sum of the reflected and diffracted fields:

$$(\mathbf{H}^S,\mathbf{E}^S) = (\mathbf{H}^R,\mathbf{E}^R) + (\mathbf{H}^D,\mathbf{E}^D) \ . \tag{1.9}$$

All three fields satisfy Maxwell's equations. In our analysis we assume that there is no diffraction, i.e. $(\mathbf{H}^D,\mathbf{E}^D) = (\mathbf{0},\mathbf{0})$. We then postulate that the reflected field has a uniformly valid asymptotic expansion of the form:

$$(\mathbf{H}^R(\mathbf{x}),\mathbf{E}^R(\mathbf{x})) \sim e^{ikS(\mathbf{x})} \sum_{n=0}^{\infty} \frac{1}{(ik)^n} (\mathbf{H}^{(n)}(\mathbf{x}),\mathbf{E}^{(n)}(\mathbf{x})) \ , \tag{1.10}$$

where $k := \omega/c$ and $c := 1/(\epsilon_0\mu_0)^{1/2}$. $(\mathbf{H}^R,\mathbf{E}^R)$ is an outgoing wave satisfying the homogeneous Maxwell's equations and radiation conditions.

It is easily shown that $S(\cdot)$, $\mathbf{H}^{(n)}$, $\mathbf{E}^{(n)}$ satisfy respectively:

$$|\nabla S|^2 = 1 \quad \text{(eikonal equation)} \tag{1.11}$$

and, along a ray:

$$2d_\gamma \mathbf{E}^{(n)} + (\nabla^2 S)\mathbf{E}^{(n)} = -\nabla^2 \mathbf{E}^{(n-1)} \tag{1.12}$$

$$2d_\gamma \mathbf{H}^{(n)} + (\nabla^2 S)\mathbf{H}^{(n)} = -\nabla^2 \mathbf{H}^{(n-1)}, \qquad n = 0,1,2,\ldots \tag{1.13}$$

with $\mathbf{H}^{(-1)} = 0$, $\mathbf{E}^{(-1)} = 0$, where:

$$d_\gamma f(\mathbf{x}(\gamma)) \equiv \nabla S(\mathbf{x}) \cdot \nabla f(\mathbf{x}(\gamma)) \tag{1.14}$$

is the differentiation along a ray.

The boundary condition (1.1) becomes:

$$-\hat{\mathbf{n}} \times \mathbf{E}^R - \mathbf{Z}(\hat{\mathbf{n}} \times \hat{\mathbf{n}} \times \mathbf{H}^R) = \hat{\mathbf{n}} \times \mathbf{E}^I - \mathbf{Z}(\hat{\mathbf{n}} \times \hat{\mathbf{n}} \times \mathbf{H}^I) \quad \text{at } \partial D \ . \tag{1.15}$$

In some special cases, e.g. with TE and TM waves, Maxwell's equations reduce to 6 scalar wave equations with uncoupled impedance BCs (Senior [6]). This was the case with

an earlier work of ours (Chen & Bridges [7]), where we considered a problem for acoustic waves. For the present problem, no such reduction is possible, hence the calculations will be more complicated.

I.4. A preliminary example: a plane wave incident on an impedance plane

To illustrate the basic role of an impedance boundary condition, the following simple example is considered. An E-polarized wave $E^I := (0,0,E_3^I)$ is incident on the (x_1,x_3)-plane, where:

$$E_3^I(x) = e^{-ik(x_1\cos\alpha+x_2\sin\alpha)}, \quad (\alpha \neq 0) . \tag{1.16}$$

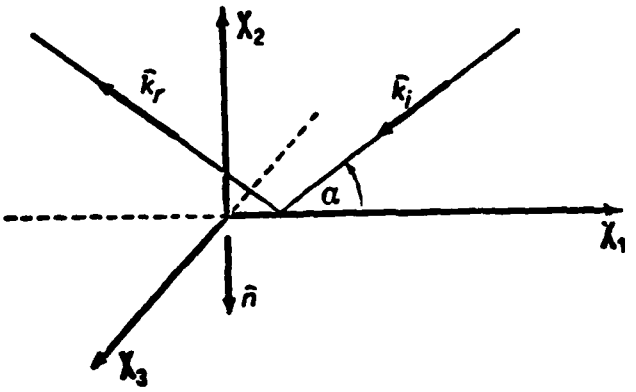

Figure 1. A plane wave incident on an impedance plane.

The $x_2 = 0$ plane is assumed to have the following boundary impedance:

$$Z = \begin{bmatrix} z & 0 & 0 \\ 0 & z & 0 \\ 0 & 0 & z \end{bmatrix}, \quad \text{Re } z > 0 . \tag{1.17}$$

A straightforward calculation based on Sections I.1 and I.2 gives the following exact solution for the reflected field:

$$E_1^R(x) = E_2^R(x) = 0; \; E_3^R(x) = \frac{\mu_0\omega - kz\sin\alpha}{\mu_0\omega + kz\sin\alpha} e^{-ik(x_1\cos\alpha-x_2\sin\alpha)}, \tag{1.18}$$

$$H_1^R(x) = -\frac{k\sin\alpha}{\mu_0\omega}\cdot\frac{\mu_0\omega - kz\sin\alpha}{\mu_0\omega + kz\sin\alpha}\,e^{-ik(x_1\cos\alpha - x_2\sin\alpha)}\,,$$

$$H_2^R(x) = -\frac{k\cos\alpha}{\mu_0\omega}\cdot\frac{\mu_0\omega - kz\sin\alpha}{\mu_0\omega + kz\sin\alpha}\,e^{-ik(x_1\cos\alpha - x_2\sin\alpha)}\,, \qquad (1.19)$$

$$H_3^R(x) = 0\,.$$

From the last expressions, the special value:

$$z = \mu_0 c/(\sin\alpha) \qquad (1.20)$$

implies that the reflected fields vanish everywhere in R_3^+. This example helps us to point out some facts, which hold in a more general context: (a) the optimal impedance, which minimizes the reflected field depends upon the angle of incidence of the incoming wave and (generally) on its frequency, (b) if we let $\alpha = \pi/2$ in (1.20), we obtain $z = (\mu_0/e_0)^{1/2}$, which does not comply with (1.6), and (c) if we assume $\mathrm{Re}\ z = (\mu_0/e_0)^{1/2} := z_0$ (the "free space" impedance, $z_0 \simeq 366.9$ Ohm), from (1.5) we get $\sigma = e\omega/2$ and $\delta_s/\lambda = 1/\pi$, i.e. the wavelength and the penetration depth are comparable, contrary to the constraint (1.7).

I.5. A spherical electromagnetic wave impinging on an impedance plane

Let an electric dipole antenna with moment $\tilde{\mathbf{p}} = (\tilde{p}_1, \tilde{p}_2, \tilde{p}_3)$ be located at the source point $x_S = (0,0,2d)$, $d > 0$. An impedance plane is located at $x_3 = d$. The reference frame and the field layout are shown in Figure 2. On the $x_3 = d$ plane the impedance boundary condition:

$$-\hat{\mathbf{n}} \times \mathbf{E} = z(\hat{\mathbf{n}} \times \hat{\mathbf{n}} \times \mathbf{H}) \qquad (1.22)$$

subject to (1.3) is satisfied. This is the example we shall consider with greater detail. In order to solve any of the minimization problems listed in Section I.1, we need the reflected fields at the observation point $x_R \in D$. These fields will be evaluated as explained in Section I.3.

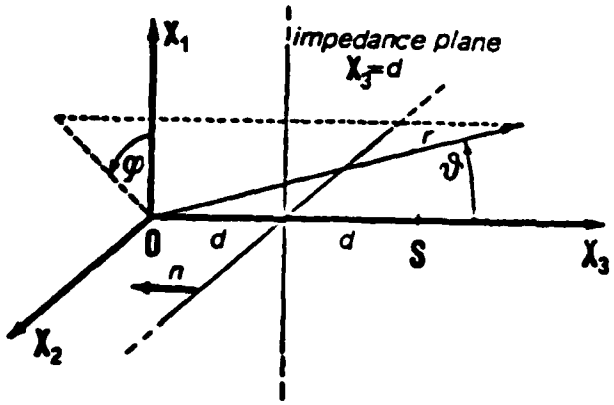

Figure 2. Impedance plane illuminated by a spherical wave. $x_1 = r \sin\theta \cos\varphi$; $x_2 = r \sin\theta \sin\varphi$; $x_3 = r \cos\theta$; boundary condition at the $(x_3 = d)$ plane: $-\hat{n} \times \mathbf{E} = z(\hat{n} \times \hat{n} \times \mathbf{H})$.

II. GEOMETRICAL OPTICS APPROXIMATIONS

II.1. The potential and the incident fields

The vector potential $\mathbf{A}$ is defined by:

$$\begin{aligned} \nabla \times \mathbf{A} &= \mu_0 \mathbf{H} , \\ \nabla \cdot \mathbf{A} &= i\omega\mu_0 e_0 \phi \quad \text{(Lorentz gauge condition)} , \end{aligned} \tag{2.1}$$

where the scalar potential ϕ satisfies:

$$\nabla\phi = -\mathbf{E} + i\omega\mathbf{A} . \tag{2.2}$$

Then $\mathbf{A}$ and ϕ satisfy a Helmholtz equation. In particular $\mathbf{A}^I$, associated to $(\mathbf{E}^I,\mathbf{H}^I)$, satisfies:

$$\begin{cases} \nabla^2\mathbf{A}^I + k^2\mathbf{A}^I = -4\pi p\delta(\mathbf{x} - \mathbf{x}_s) \\ \text{radiation conditions} . \end{cases} \tag{2.3}$$

The solution to (2.3) (fundamental solution or free space Green's function) reads:

$$\mathbf{A}^I = pe^{ikr^*}/r^* , \tag{2.4}$$

where $r^* := |\mathbf{x}^*| = |\mathbf{x} - \mathbf{x}_s| = [x_1^2 + x_2^2 + (x_3 - 2d)^2]^{1/2}$ and $\mathbf{p} = -i\omega\mu_0\bar{\mathbf{p}}/4\pi$. We are thus modelling a dipole antenna emitting spherical waves. The associated incident fields at any point $\mathbf{x} \in D$, $\mathbf{x} \neq \mathbf{x}_s$, are:

$$\mathbf{H}^I = (1/\mu_0)\nabla \times \mathbf{A} = (\hat{\mathbf{x}} \times \mathbf{p})(e^{ikr^*}/\mu_0 r^*)(1 - 1/ikr^*) \tag{2.5}$$

$$\mathbf{E}^I = (i/e_0\omega)\nabla \times \mathbf{H}^I , \tag{2.6}$$

where $\hat{\mathbf{x}}^* := (\mathbf{x} - \mathbf{x}_s)/|\mathbf{x} - \mathbf{x}_s| = \hat{\mathbf{x}}^*/r^*$. (See e.g. Jackson, [8], §9.2).

II.2. The boundary condition

Since the reflected wave is also spherical, then by Snell's law it diverges from a virtual point source, which, as Figure 2 shows, is located at the origin. Two geometries, spherical and planar, are involved in the boundary condition. Since $\hat{\mathbf{n}} = (0,0,-1)$, (1.15) and (1.22) yield two scalar equations:

$$\begin{cases} z\mathbf{E}_1^R - \mathbf{E}_2^R = -z\mathbf{H}_1^I + \mathbf{E}_2^I := b_1 \\ z\mathbf{E}_2^R - \mathbf{E}_1^R = -z\mathbf{H}_2^I - \mathbf{E}_1^I := b_2 , \end{cases} \tag{2.7}$$

which are not sufficient to find $(\mathbf{E}^R,\mathbf{H}^R)$. They must be completed by an independent

scalar equation, i.e.

$$\nabla \cdot \mathbf{E}^R = 0 \ . \tag{2.8}$$

Since b_1 and b_2 in (2.7) are known functions, obtained from (2.5) and (2.6), and since $\mathbf{E}^R$ can be written in terms of $\mathbf{H}^R$, (2.7) becomes:

$$\begin{cases} ikzh_1 + z_0(\partial_3 h_1 - \partial_1 h_3) = b_1 \\ ikzh_2 - z_0(\partial_2 h_3 - \partial_3 h_2) = b_2 \ , \end{cases} \quad \text{at} \quad x_3 = d, \ \forall x_1, x_2 \tag{2.9}$$

where:

∂_i denotes the partial derivative w.r. to x_i, $i = 1,2,3$;

h_i denotes the reflected magnetic field components;

z_0 has been defined in Section I.4.

II.3. Geometrical optics expansion

Expansion (1.10) for the reflected magnetic field becomes:

$$\begin{bmatrix} h_1 \\ h_2 \\ h_3 \end{bmatrix} = ik \, e^{ikr} \sum_{n=0}^{\infty} (ik)^{-n} \begin{bmatrix} u_n \\ v_n \\ w_n \end{bmatrix} \ , \qquad r > d \ , \tag{2.10}$$

since $S(x) = r$, the coordinate along a ray being r. For convenience we have factored ik out of the sum. By (2.10) a system of partial differential equations (2.8, 2.9) is transformed into an algebraic system, which is solved by the identity principle. The expressions of b_1 and b_2 are polynomials containing powers of (ik). Then the sets of equations for (u_n, v_n, w_n) will be obtained by equating the coefficients of given powers of (ik). Let us begin with $n = 0$: by introducing polar coordinates (see caption of Figure 2 for the notations) the following system is obtained:

$$\begin{cases} (z_0\cos\theta + z)u_0 - z_0\sin\theta\cos\varphi w_0 = b_{01} \\ (z_0\cos\theta + z)v_0 - z_0\sin\theta\sin\varphi w_0 = b_{02}, \quad x_3 = d, \ \forall x_1, x_2 \\ \sin\theta\cos\varphi u_0 + \sin\theta\sin\varphi v_0 + \cos\theta w_0 = 0 \ , \end{cases} \tag{2.11}$$

where:

$$b_{01} := (1/\mu_0 r_p)(z_0\cos\theta - z)(p_3\sin\theta\sin\varphi + p_2\cos\theta) + z_0\sin^2\theta\cos\varphi(p_2\cos\varphi - p_1\sin\varphi);$$

$$b_{02} := (1/\mu_0 r_p)(z - z_0\cos\theta)(p_3\sin\theta\cos\varphi + p_1\cos\theta) + z_0\sin^2\theta\sin\varphi(p_2\cos\varphi - p_1\sin\varphi);$$

$$r_p := (x_1^2 + x_2^2 + d^2)^{1/2} = d/\cos\theta \ .$$

From (2.11) we get the 0th order component of the reflected magnetic field at $x_3 = d$, $\forall x_1, x_2$:

$$u_0 = (UQ - SPX)/\mu_0 r_p V; \ v_0 = -(UR + TPX)/\mu_0 r_0 V; \ w_0 = YP\sin\theta/\mu_0 r_p \qquad (2.12)$$

where:

$$P := p_1\sin\varphi - p_2\cos\varphi \qquad Q := p_3\sin\theta\sin\varphi + p_2\cos\theta$$

$$R := p_3\sin\theta\cos\varphi + p_1\cos\theta \qquad S := z_0\sin^2\theta\cos\varphi$$

$$T := z_0\sin^2\theta\sin\varphi \qquad U := z_0\cos\theta - z$$

$$V := z_0\cos\theta + z \qquad X := 2z\cos\theta/(z_0 + z\cos\theta)$$

$$Y := (z_0 - z\cos\theta)/(z_0 + z\cos\theta) \ . \qquad (2.13)$$

The result stated by (2.12) can be extended $\forall x_3 > d$ by integrating the transport equation (1.13). This is a straightforward step for $n = 0$ only, since then the right-hand-side is 0. The required field components are obtained by replacing r_p by r in (2.12), where $r := (x_1^2 + x_2^2 + x_3^2)^{1/2}$, $x_3 > d$.

The 0th-order reflected electric field components are derived from (2.12) and the counterpart of (2.6), by applying the identity principle. In analogy with (2.10) they are denoted by (ξ_0, η_0, ζ_0) and read:

$$\xi_0 = z_0(v_0\cos\theta - w_0\sin\theta\sin\varphi)$$

$$\eta_0 = -z_0(u_0\cos\theta - w_0\sin\theta\cos\varphi), \quad \forall x \in D \qquad (2.14)$$

$$\zeta_0 = z_0\sin\theta(u_0\sin\varphi - v_0\cos\varphi) \ .$$

In order to obtain higher order components, we may follow the already mentioned procedure of applying the identity principle to the algebraic system and solving the corresponding transport equations. This leads to very complex calculations. An alternative approach is suggested by the symmetry properties of the generalized spherical waves appearing in (2.10). By applying a result due to Keller, Lewis, Seckler [9], it can be easily shown that

$$\begin{bmatrix} u_1 \\ v_1 \\ w_1 \end{bmatrix} = (1/2r)B \begin{bmatrix} u_0 \\ v_0 \\ w_0 \end{bmatrix} , \tag{2.15}$$

where the Beltrami operator $B(\cdot)$ is defined by:

$$B(\cdot) := (\sin\theta)^{-1}(\partial_\theta \sin\theta \partial_\theta(\cdot) + (1/\sin\theta)\partial^2_{\varphi\varphi}(\cdot)) . \tag{2.16}$$

In our case it can be shown that none of the quantities dealt with are singular at $\theta = 0$. The action of $B(\cdot)$ on the components given by (2.12) yields:

$$Bu_0 = \partial^2_{\theta\theta}u_0 - \{[z_0Q + P(S'_\theta X + S'X_\theta)]\cos\theta - 2X(S''_\varphi P_\varphi + S''P) + UQ\} \cdot$$
$$\cdot (1/\mu_0 rV) + z_0(UQ - SPX)/\mu_0 rv^2 , \tag{2.17}$$

$$Bw_0 = \partial^2 w_0 + [(Y_\theta P + YP_\theta)\cos\theta - YP\sin^2\theta]/\mu_0 r , \tag{2.18}$$

where the subscripts θ and φ denote the partial derivative with respect to said variables, the prime (') denotes division by $\sin\theta$ and the double prime (") division by $\sin^2\theta$. Similarly Bv_0 is obtained from (2.17) by orderly replacing (u_0,Q,S) by $(v_0,-R,T)$ and their partial derivatives.

Finally, the 1st order components of the reflected electric field are written as functions of the already calculated 0th and 1st order reflected magnetic field components and of their partial derivatives with respect to polar coordinates:

$$\begin{aligned}
\xi_1(r,\theta,\varphi) &= \sqrt{\frac{\mu_0}{\varepsilon_0}} \left(v_1\cos\theta - w_1\sin\theta\sin\varphi + \cos\theta \frac{\partial v_0}{\partial r} - \frac{\sin\theta}{r}\frac{\partial v_0}{\partial\theta}\right. \\
&\quad \left. - \sin\theta\sin\varphi \frac{\partial w_0}{\partial r} - \frac{\cos\theta\sin\varphi}{r}\frac{\partial w_0}{\partial\theta} - \frac{\cos\varphi}{r\sin\theta}\frac{\partial w_0}{\partial\varphi}\right) \\
\eta_1(r,\theta,\varphi) &= \sqrt{\frac{\mu_0}{\varepsilon_0}} \left(-u_1\cos\theta + w_1\sin\theta\cos\varphi - \cos\theta \frac{\partial u_0}{\partial r} + \frac{\sin\theta}{r}\frac{\partial u_0}{\partial\theta}\right. \\
&\quad \left. + \sin\theta\cos\varphi \frac{\partial w_0}{\partial r} + \frac{\cos\theta\cos\varphi}{r}\frac{\partial w_0}{\partial\theta} - \frac{\sin\varphi}{r\sin\theta}\frac{\partial w_0}{\partial\varphi}\right) \\
\zeta_1(r,\theta,\varphi) &= \sqrt{\frac{\mu_0}{\varepsilon_0}} \left(u_1\sin\theta\sin\varphi - v_1\sin\theta\cos\varphi + \sin\theta\sin\varphi \frac{\partial u_0}{\partial r} + \frac{\cos\theta\sin\varphi}{r}\frac{\partial u_0}{\partial\theta}\right. \\
&\quad \left. + \frac{\cos\varphi}{r\sin\theta}\frac{\partial u_0}{\partial\varphi} - \sin\theta\cos\varphi \frac{\partial v_0}{\partial r} - \frac{\cos\theta\cos\varphi}{r}\frac{\partial v_0}{\partial\theta} + \frac{\sin\varphi}{r\sin\theta}\frac{\partial v_0}{\partial\varphi}\right) .
\end{aligned} \tag{2.19}$$

It may be interesting at this point to make a comparison between the asymptotic expansion we have chosen and other approximations, known as the paraxial and Fresnel's approximations, also frequently used in electromagnetics. In our case we have started with the fundamental solution (2.4) and approximated the reflected fields by the 0th and 1st order terms in the expansion (2.10), which is acceptable whenever $kr \gg 1$. On the other hand the paraxial and Fresnel's approximations, the equivalence of which has been discussed by Crosta [10] for a scalar case, apply if the fundamental solution is known in closed form and affects phase factors appearing in the complex exponential propagator. Closed form fundamental solutions are easily obtained when boundary conditions are of the Dirichlet or Neumann type, and yield the well-known Rayleigh-Sommerfeld propagators. The solution corresponding to impedance BCs for the scalar case has been given by Malyughinetz [11]. In this paper the implementation of Malyughinetz's results will not be considered.

III. FINDING THE OPTIMAL SURFACE IMPEDANCE VALUE

III.1. Problem statement

Let us assume that the surface impedance can take on values belonging to either of the following sets:

$$Z_{ad}^{u} := \{z \in \mathbb{C} \mid 0 < \rho_1 \leq \mathrm{Re}\ z \leq \rho_2,\ |z| \leq b\} \tag{3.1}$$

and

$$Z_{ad}^{c} := \{z \in Z_{ad}^{u} \mid \mathrm{Re}\ z = \mathrm{Im}\ z\}\ , \tag{3.2}$$

hereinafter named "the admissible sets" and denoted by Z_{ad}, whenever no ambiguity arises. Equation (3.1) contains in particular the positivity constraint for Re z; (3.2) represents the physical realizability constraint, discussed in §I.2.

Let χ denote the index function of Z_{ad}, which is 0 if $z \in Z_{ad}$ and $+\infty$ elsewhere; then we define the objective functions J_m, $m = 1,\ldots,4$:

$$J_1(z) := \frac{1}{2}\left(\epsilon_0 \mathbf{E}_R^*(x) \cdot \mathbf{E}_R(x) + \mu_0 \mathbf{H}_R^*(x) \cdot \mathbf{H}_R(x)\right) + \chi|z| = W_1 + \chi|z|\ , \tag{3.3}$$

$$J_2(z) := \int_V W_1 dV + \chi|z| := W_2 + \chi|z|\ , \tag{3.4}$$

$$J_3(z) := \frac{1}{2}\left|\mathbf{E}_R(x) \times \mathbf{H}_R^*(x)\right|^2 + \chi|z| := W_3 + \chi|z|\ , \tag{3.5}$$

$$J_4(z) := \frac{1}{2}\int_\Sigma \mathrm{Re}[\mathbf{E}_R(x) \times \mathbf{H}_R^*(x)] \cdot \hat{n} d\Sigma + \chi|z| := W_4 + \chi|z|\ . \tag{3.6}$$

Each of the J_m's is the sum of a "physical" term, W_m, and of an "economical" one, $\chi|z|$; the purpose of the latter will be clarified at the end of this subsection. The term W_1 is the time averaged reflected energy density at $x = (r,\theta,\varphi) \in D$, while W_2 results from integrating W_1 over a bounded domain $V \subset\subset D$; W_3 is the time averaged squared modulus of the reflected Poynting vector $\mathbf{S}_R(x)$; W_4 is the flux of $\mathrm{Re}(\mathbf{S}_R)$ through a given bounded surface Σ, s.t. $\Sigma \cap \partial D = \emptyset$.

The J_m's depend on z through the fields.

We now state the minimization problem:

find the surface impedance $\hat{z} \in Z_{ad}$, which minimizes one of the J_m's, i.e.:

$$J_m(\hat{z}) = \min_{Z_{ad}} J_m(z);\ m \text{ given}\ . \tag{3.7}$$

This problem will be solved by an iterative procedure, which consists of the steps also shown by Figure 3:

1 - set $k = 0$;

2 - given $z^k \in Z_{ad}$, determine the reflected fields to the desired order of approximation (one, in our case);

3 - compute W_m^k, i.e. J_m^k, since $z^k \in Z_{ad}$;

4 - from J_m^k and its derivative w.r. to z, J_{mz}^k, defined in §III.2, determine $z^{k+1} \in Z_{ad}$ s.t. $J_m^{k+1} < J_m^k$;

5 - repeat the whole procedure from step n.2 until some stopping condition is met.

In detail, step n.2 requires the solution of a control problem, described by the map:

$$T : Z_{ad} \text{ -----> } (C^\infty(D))^3 \times (C^\infty(D))^3 := X \qquad (3.8)$$

$$z \text{ -----> } (\mathbf{E}_R, \mathbf{H}_R)$$

where T is a $C^\infty(Z_{ad})$ diffeomorphism and z is the input.

Step n.3 is related to observation of the system, since $W_m(\cdot)$ is an observation map and $W_m(z)$ is the output.

Step n.4 consists of updating the input according to the observed quantity; in other words information is feedback from output to input.

Among the stopping conditions appearing in step n.5 the following are considered:

- an upper bound on the number of iterations, k
- a lower bound, $J_{m(min)}$, for the objective function
- a lower bound, $|J_{mz(min)}|$, for the modulus of the derivative (see §III.2).

Without going into further details, we point out that both analytical and physical considerations play a role in determining $J_{m(min)}$. Let us assume that the minimum detectable energy in a given V is known: this value may then be assigned to $J_{2(min)}$. From an analytical viewpoint, $J_{m(min)}$ can be related to the modelling error, which affects all field functions, since (2.10) and its counterpart for the electric field are replaced by the sum of the first two terms. With reference to W_1, $J_{1(min)}$ is chosen as the best upper bound of the energy density due to the neglected terms ($n > 2$ in (2.10)).

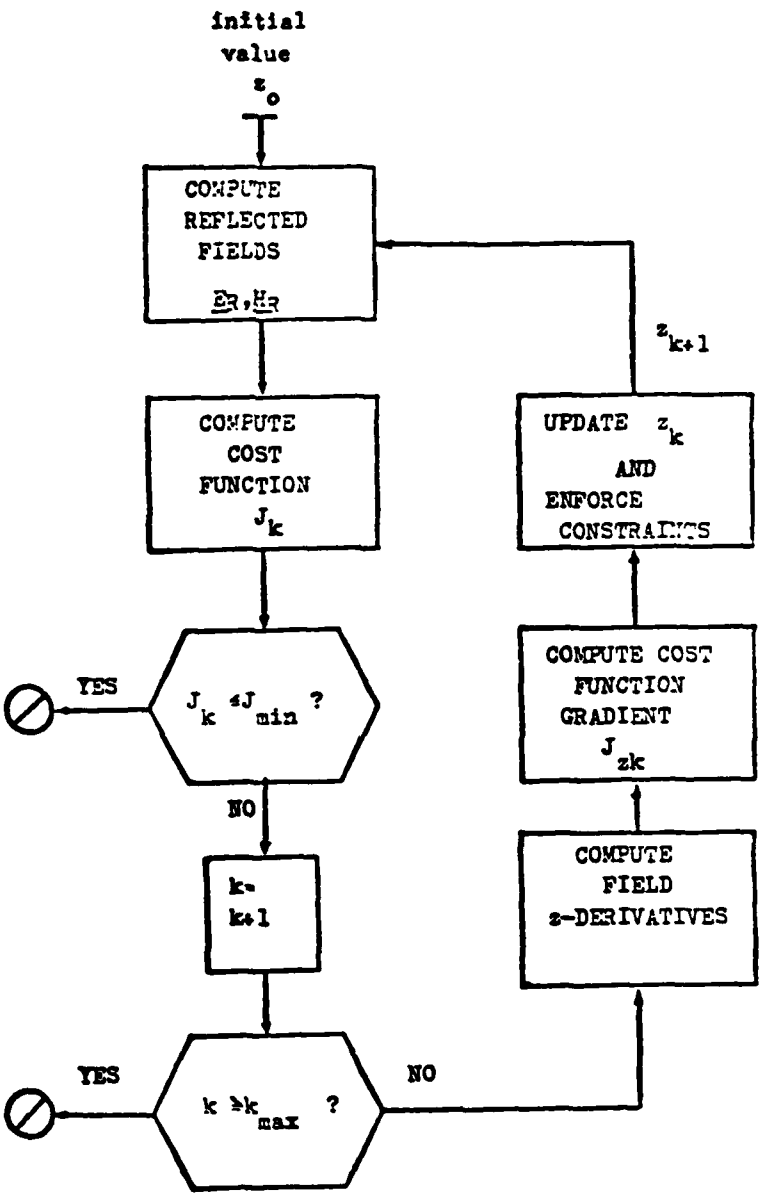

Figure 3. Block diagram of the steepest descent constrained minimization algorithm where k is the iteration number.

We now consider the well-posedness of the minimization problem.

Existence of at least one $\hat{z}$ is insured by the economical term defined above. Moreover, $\hat{z}$ continuously depends on the problem parameters, e.g. the observation point coordinates, because T of (3.8) is smooth and all of the J_m's are continuous functions of z in Z_{ad}.

Uniqueness of $\hat{z}$ cannot be proved in a straightforward way. Other properties of $\hat{z}$ appear when the first order derivatives of J_m's are studied.

III.2. The derivatives of J_m w.r. to z

We notice that all of the J_m's are continuous real valued functions of a complex quantity, z, where a field vector and its complex conjugate always appear together. Since $\mathbf{E}(\cdot)$ depends on z alone and $\mathbf{E}^*(\cdot)$ depends on z^*, then it makes sense to consider both z and z^* as independent variables.

Let us denote by $\mathbf{E}_z$ the derivative of $\mathbf{E}$ w.r. to z; then the first variation of $W_1(\cdot)$ reads:

$$dW_1 = \frac{1}{2}\left[\epsilon_0(\mathbf{E}^* \cdot \mathbf{E}_z dz + \mathbf{E}^*_{z^*} \cdot \mathbf{E}\, dz^*) + \mu_0(\mathbf{H}^* \cdot \mathbf{H}_z + \mathbf{H}^*_{z^*} \cdot \mathbf{H}\, dz^*)\right] =$$

$$= \mathrm{Re}(J_{1z})d\rho - \mathrm{Im}(J_{1z})d\tau \,, \tag{3.9}$$

where:

$$J_{1z} := \epsilon_0 \mathbf{E}^* \cdot \mathbf{E}_z + \mu_0 \mathbf{H}^* \cdot \mathbf{H}_z \,. \tag{3.10}$$

Similar expressions are obtained for the other physical terms; in particular

$$J_{3z} = \mathbf{S} \cdot (\mathbf{E}^* \times \mathbf{H}_z) - \mathbf{S}^* \cdot (\mathbf{H}^* \times \mathbf{E}_z) \,, \tag{3.11}$$

$$J_{4z} = (\mathbf{E}_z \times \mathbf{H}^* + \mathbf{E}^* \times \mathbf{H}_z) \cdot \hat{\mathbf{n}} \,, \tag{3.12}$$

where each of the J_{mz}'s is a complex quantity, hereinafter called the "gradient" of J_m w.r. to z. The differential properties of J_m lead to the following result:

let $z \in Z_{ad}$, then $Z = 0$ is a locus of stationary points of J_m (for any m), which are either relative maxima or minima.

The proof is straightforward: from the definitions (3.3) to (3.6) we get $J(z) = J(z^*)$, where we have dropped the subscript m for simplicity. For a given $\tilde{\rho}$

away from the boundary of Z_{ad}^{u} we have $J(\tilde{\rho};\tau) = J(\tilde{\rho};-\tau)$; since $J(\cdot;\cdot)$ is at least of class C^1 w.r. to τ, then $dJ(\tilde{\rho};\tau) = -dJ(\tilde{\rho};-\tau)$; in particular $dJ(\tilde{\rho};0) = 0$.

Second order analysis is needed in general to tell whether at $(\tilde{\rho};0)J(\tilde{\rho};0)$ attains a local maximum or minimum. If we deal e.g. with $J_1(\cdot)$ and consider the analogy between the reflection of spherical waves and the preliminary example of §I.4, we could easily show, without performing any computation, that real values of z must yield local <u>minima</u> of J_1. This intuitive conclusion is supported by a study of the Hessian matrix of J_1, denoted by $\nabla^2 J_1$, and defined by:

$$\nabla^2 J_1 := \begin{bmatrix} J_{zz} & J_{zz^*} \\ J_{z^*z} & J_{z^*z^*} \end{bmatrix}, \tag{3.13}$$

where J_{zz} stands for the 2^{nd} order derivative of J_1 w.r. to z. The 2^{nd} order variation d^2J_1 of J_1 then reads:

$$d^2J_1 = (dz\ dz^*)(\nabla^2 J_1)\begin{pmatrix} dz \\ dz^* \end{pmatrix}, \tag{3.14}$$

alternatively, it can be expressed in terms of $(d\rho, d\tau)$:

$$d^2J_1 = (d\rho\ d\tau) \cdot \mathbf{T}^{trs} \cdot \nabla^2 J_1 \cdot \mathbf{T} \cdot \begin{pmatrix} d\rho \\ d\tau \end{pmatrix} \tag{3.15}$$

where $\mathbf{T} := \begin{bmatrix} 1 & i \\ 1 & -i \end{bmatrix}$ and $\mathbf{T}^{trs}$ denotes the transpose of $\mathbf{T}$. Let us now define $\hat{\mathbf{H}} := \mathbf{T}^{trs} \cdot \nabla^2 J_1 \cdot \mathbf{T}$; then the eigenvalues of $\hat{\mathbf{H}}$, λ_1 and λ_2, read:

$$\lambda_{1,2} = J_{zz^*} \mp |J_{zz}| . \tag{3.16}$$

They are always <u>real</u>. Numerical computation is needed to evaluate them (see §§III.4 and III.5.4). At $\tau = 0$, $\forall \rho \in Z_{ad}$ they are both strictly positive, hence $\tau = 0$ is a locus of relative <u>minima</u> for J_1.

III.3. <u>The minimization algorithm</u>

The algorithm introduced in §III.1 is implemented on the discretized counterpart of the original minimization problem. The rule which yields $z^{k+1} \in Z_{ad}$ at step n.4

characterizes the steepest descent method with projection (Giannessi [12]; Pchénitchny & Daniline [13] and reads:

$$z^{k+1} = P_{Zad}(z^k - t^k \cdot (J_z^k)^*) \ , \tag{3.17}$$

where:

J_z^k is a function of the fields evaluated at the k-th iteration, according to (3.10) and the like;

t^k is the updating step, chosen between the following quantities:

$$t^k = \min(J^k/|J_z^k|^2;\ |J_z^k|^{-1}) \ , \tag{3.18}$$

P_{Zad} is the projection operator on Z_{ad}, which enforces all constraints implied either by (3.1) or by (3.2).

To assess the convergence of the $\{z^k\}$ sequence obtained from (3.17) we may apply a theorem by Pchénitchny & Daniline ([13], p. 48). Let $G \subseteq Z_{ad}$ be a subdomain where the eigenvalues defined by (3.16) satisfy $\lambda_2 > \lambda_1 > 0$. We define:

$$\begin{aligned} \lambda_L &:= \min_G \lambda_1(\rho,\tau) \ , \\ \lambda_U &:= \max_G \lambda_2(\rho,\tau) \ . \end{aligned} \tag{3.19}$$

then:

$$|z^{k+1} - z^k| \leq |z^0 - \hat{z}| \cdot |2\lambda_U/(\lambda_U - \lambda_L)| \cdot (\lambda_U/\lambda_L)^{1/2} \cdot ((\lambda_U - \lambda_L)/(\lambda_U + \lambda_L))^{k+1} \ . \tag{3.20}$$

On the other hand, if $\lambda_L \leq 0$, no general convergence property holds.

III.4. Structure of the computer code

A computer code which implements the theory presented so far has been written in the FORTRAN ASCII language and developed on the Univac 1100/90 owned by CILEA at Segrate (Milan, Italy).

In order to handle fields and their functions a suitable system of units is chosen, s.t.

the wavelength, λ, is the new unit of length,

vacuum permittivity ϵ_0 and magnetic permeability μ_0 take on unit values,

z values are normalized to the free space impedance $z_0 := (\mu_0/\epsilon_0)^{1/2}$.

Data are supplied by the user in MKSA units, then automatically scaled. The computed functions of the fields are printed out in MKSA units, z values are not scaled back. The reference frame can be either centered at the source (S) or at the mirror image (O) w.r. to the impedance plane. Coordinates can be supplied either in cartesian or polar form.

The problem types which can be solved are:

- "direct", i.e. computation of the discretized counterpart of J_m in a given $(\rho;\tau)$ domain contained in Z_{ad};
- "stealth", i.e. computation of $\hat{z}$ defined by (3.7);
- some utility functions: a) computation of Hessian eigenvalues according to (3.16) for given observation point and z values; b) computation of the reciprocal condition number $\mu := \lambda_1/\lambda_2$.

In connection with point observation, either J_1 (see 3.3) or J_3 of (3.5) can be chosen. If J_2 (see 3.4) is to be computed, the user must specify the integration volume. Up to now the choice is restricted to volumes enclosed between two spherical caps centered at O, which are completely defined by 6 parameters, i.e., see Figure 4:

$$V := \{(r,\theta,\varphi) | r_1 \leq r \leq r_2;\ \theta_1 \leq \theta \leq \theta_2;\ \varphi_1 \leq \varphi \leq \varphi_2\} \ . \tag{3.21}$$

A similar constraint holds for the integration surface Σ, on which J_4 of (3.6) is defined.

As soon as coordinates are read in, it is checked that d, the distance from the source S to the impedance plane, is larger than 100λ and that every observation point lies in D.

If a "direct" problem is set, the corresponding value of J_m is computed for as many times as required by the user, who enters the upper and lower values of ρ and τ and the number of parts into which both intervals must be divided.

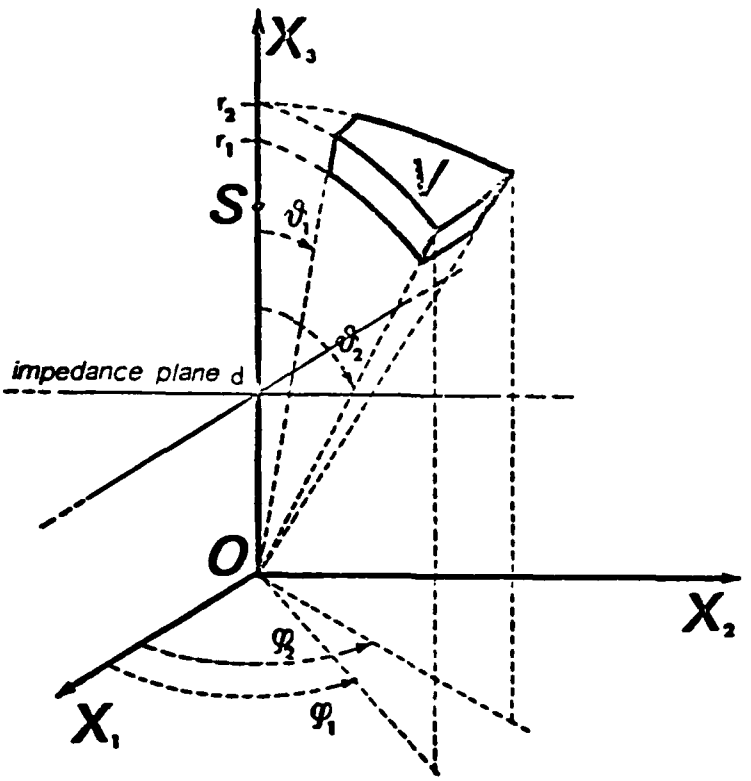

Figure 4. A typical integration volume related to J_2.

If a "stealth" problem is specified, the admissible set, (3.1) or (3.2) must be chosen; then z^0 and some more parameters must be given. For simplicity, minimization in Z^u_{ad} and in Z^c_{ad} will be referred to hereinafter by "unconstrained" and "constrained" respectively.

Numerical integration implied by (3.4) and (3.6) is performed by the KOROBO routine, based on optimal partitioning of the integration domain, due to Zakrzewska et al. [14].

Minimization is carried out as described in §III.3. Actually the rule based on (3.18) is chosen in a fast search phase. If the updated value z^{k+1} of (3.17) is not in Z_{ad}, or if $J(z^{k+1}) > J^k$, then a slow search is performed, by which J^k is locally approximated by a parabola, as described by Lemarechal [15]. Function gradients needed at

every minimization step are evaluated numerically from the field component derivatives w.r. to z, which are obtained from (2.12) to (2.19) and lead to the procedure shown in Table I. Second order z derivatives of J_1, which we do not show here for simplicity, are also needed to evaluate $\lambda_{1,2}$ of (3.16).

Table 1. The computation of a field component z-derivative as implemented in the code

Define:

$$E_z := e^{ikr}\left\{ ik\begin{pmatrix}\xi_{0z}\\ \eta_{0z}\\ \zeta_{0z}\end{pmatrix}+\begin{pmatrix}\xi_{1z}\\ \eta_{1z}\\ \zeta_{1z}\end{pmatrix}\right\} .$$

Consider the 1st component, ξ_z:

$$\xi_{0z} = v_{0z}\cos\theta - w_{0z}\sin\theta\sin\varphi$$

$$\xi_{1z} = (v_{1z} - v_{0z} \cdot r^{-1})\cos\theta - (w_{1z} - w_{0z} \cdot r^{-1})\sin\theta\sin\varphi -$$

$$- (v_{0z\theta}\sin\theta + w_{0z\theta}\cos\theta\sin\varphi) \cdot r^{-1} - (w'_{0z\varphi}\cos\varphi) \cdot r^{-1} ,$$

where (see (2.13))

$$v_{0z} = [(R - TPX_z) \cdot r^{-1} - v_0)] \cdot v^{-1} ;$$

$$w_{0z} = PY_z \cdot r^{-1} \cdot \sin\theta ;$$

$$v_{1z} = [(-2\tilde{D}v^{-1} + \tilde{D}_z - \tilde{C}) \cdot v^{-1} + \tilde{C}_z] \cdot (1/r^2 v) .$$

Explicitly:

$$\tilde{C} = -U_{\theta\theta}R - 2R_\theta U_\theta + 2UR - P(T_{\theta\theta}X + 2T_\theta X_\theta + X_{\theta\theta}T) + 2X(T''P - S''P_\varphi) +$$

$$+ [R - P(T'_\theta X + X_\theta T'))]\cos\theta ;$$

$$\tilde{D} = 2U_\theta[U_\theta R + UR_\theta + P(XT_\theta + X_\theta T)] - (UR + PXT) \cdot (1 + 2U_\theta^2 v^{-1} - U_{\theta\theta}) ,$$

from which $\tilde{C}_z, \tilde{D}_z$ are obtained.

Note: The subscript denotes the partial derivative w.r.t. the corresponding variable; the prime (') division by $\sin\theta$, the double prime (") division by $\sin^2\theta$. No quantity is singular at $\theta = 0$.

Computational results are written out, when applicable, as printer graphs or as data files, which can be further processed by a graphics package, as we shall show in the next Section.

III.5. Some computational results

Remark: All numerical values are given in MKSA units and all computations have been carried out in single precision arithmetics.

III.5.1. Symmetry properties of J_1

The following symmetry properties of J_1 are easily verified and numerically checked:

$$J_1(\theta = 0;\ \mathbf{p} = (1,0,0)) = J_1(\theta = 0;\ \mathbf{p} = (0,1,0)),\ \forall \lambda, d, r, \varphi,\ \forall z \in Z_{ad}\ , \tag{3.22}$$

$$J_1(\theta = 1;\ \varphi = \pi;\ \mathbf{p} = (0,1,0)) = J_1(\theta = 1;\ \varphi = \pi/2;\ \mathbf{p} = (1,0,0)),\ \forall \lambda, d, r,\ \forall z \in Z_{ad}\ . \tag{3.23}$$

Polarization effects are easily evaluated numerically. As expected, if $\theta \neq 0$, the direction of $\mathbf{p}$ affects J_1. E.g. for $\lambda = 1$, $d = 100$, $r = 200$, $\theta = 1$ rad, $\varphi = 0$, $\rho = \tau = 300$ ohm, $\mathbf{p} = (1,0,0)$ yields $J_1 = 1.11E + 2$ J/m^3, whereas $\mathbf{p} = (0,1,0)$ yields $J_1 = 1.35E + 2$.

III.5.2. Direct problem solutions

Figure 5 shows that the minimum of J_1 at $\tau = 0$ shifts to lower values of ρ as θ increases from 0 to 1 rad.

Table II gives the values of z (ohm) which yield the minimum and maximum of J_1 in the specified domain. The uncertainty of the values depends on z - domain discretization. More accurate figures are obtained by minimizing J_1, as discussed in §III.5.3.

The other objective functions are studied in a similar way. Results are shown by Figures 6, 7, 8.

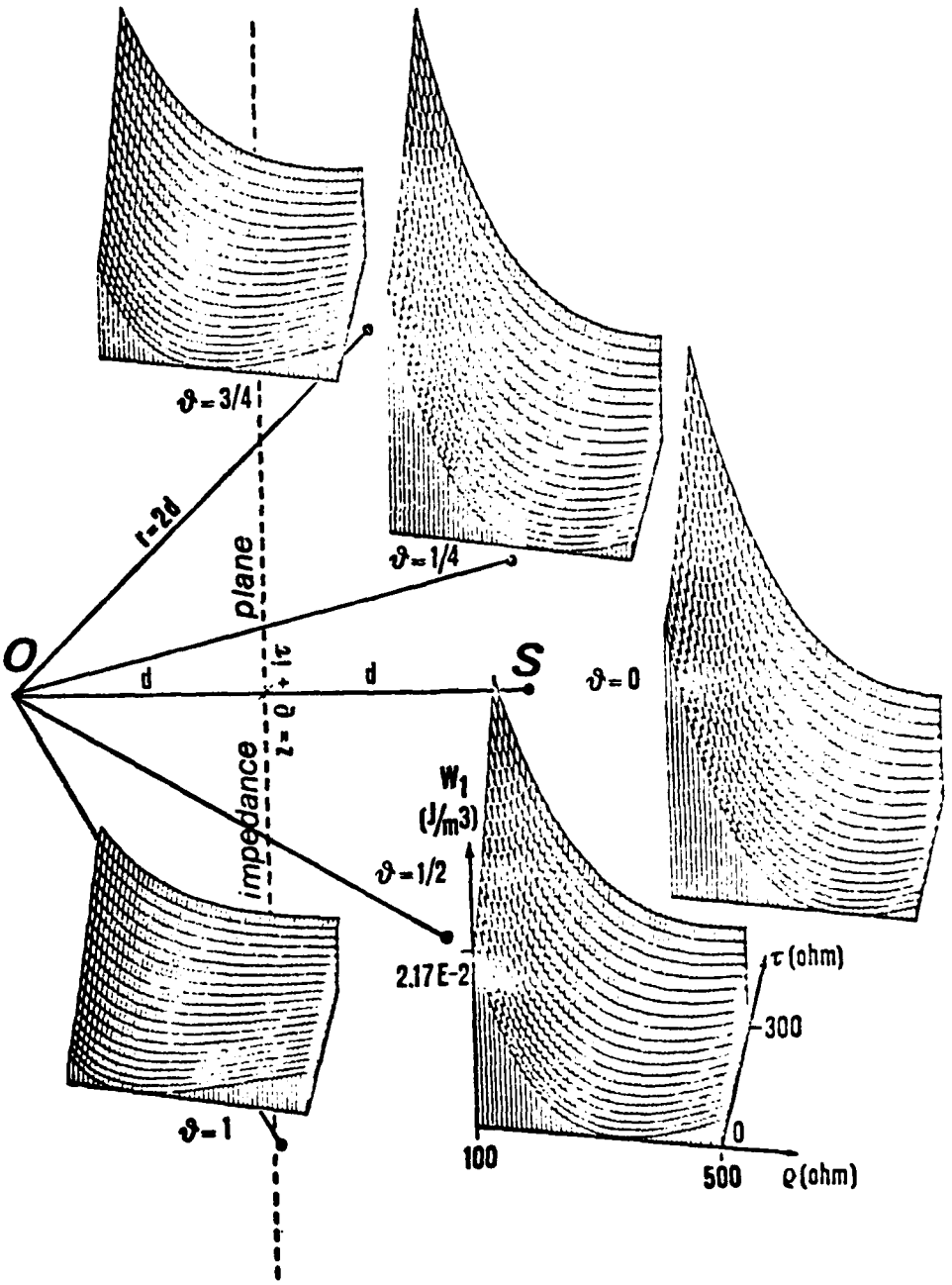

Figure 5. Energy density W_1 as a function of $(\rho;\tau)$ for some values of θ. In all cases λ = 1m; d = 100m; r = 2d; φ = 0; **p** = (1,0,0) Vs; $100 \leq \rho \leq 500$ ohm; $0 \leq \tau \leq 300$ ohm. Some relevant values of $w_1(\rho,\tau;\theta)$ are given by Table II.

Table II. Some results yielded by the direct problem solver applied to W_1

$\lambda = 1m$; $d = 100m$; $r = 200m$; $\varphi = 0$ rad.

$10^{-3} \leq \rho \leq 100$; $0 \leq \tau \leq 300$ ohm

θ (rad)	W_{1min} at (ρ (J/m^3)	τ) (ohm)	(ρ	τ)	W_{1max} at (ρ (J/m^3)	τ) (ohm)	(ρ	τ) (ohm)
0	< 5E - 7	376 ± 9	0.0		.51E - 3	100.		300.
1/4	< 5E - 7	366 ± 9	0.0		.47E - 3	100.		300.
1/2	< 5E - 7	328 ± 9	0.0		.38E - 3	100.		300.
3/4	< 5E - 7	270 ± 9	0.0		.27E - 3	100.		300.
1	< 5E - 7	204 ± 9	0.0		.16E - 3	100.		300.

The typical CPU time needed to compute 484 values of J_1 or J_3 is 0.45 s. It becomes about 30 times longer when J_2 or J_4 are processed, because the above mentioned integration routine must be called.

III.5.3. Minimization of the objective functions

Tables III and IV refer to the minimization of J_1. The terms "unconstrained" and "constrained" have been defined in §III.4. We notice that the machine precision limit is achieved in the "unconstrained" case, typically after 30 iterations. Given $z^0 = 100$ ohm, the convergence of $\{z^k\}$ towards $\hat{z}_{exact}$ is s.t. $|z^k - \hat{z}_{exact}|/(z_{exact}) < 10^{-4}$ for $k > 16$.

In order to determine $\hat{z}$ in the "constrained" case ($\rho = \tau$), the example of §I.4 is again of some help. If we set $\alpha = \pi/2$ in (1.18), (1.19) and consider the minimization of $\mathbf{H}_R \cdot \mathbf{H}_R^*$, to which J_1 of (3.3) is proportional, we get:

$$\hat{\rho} = z_0/\sqrt{0} \ . \tag{3.24}$$

In passing we note that $\delta_s/\lambda = 1/\pi\sqrt{2}$ in this case. The $\hat{z}$ value just given must be compared to the computed ones in line 1, columns 3 and 5 of Table III and with the whole

column 8 of Table IV. Convergence speed of $\{z^k\}$ is similar to that of the "unconstrained" case. Values of $\hat{\rho}$ for different observation angles cannot be determined with equal ease.

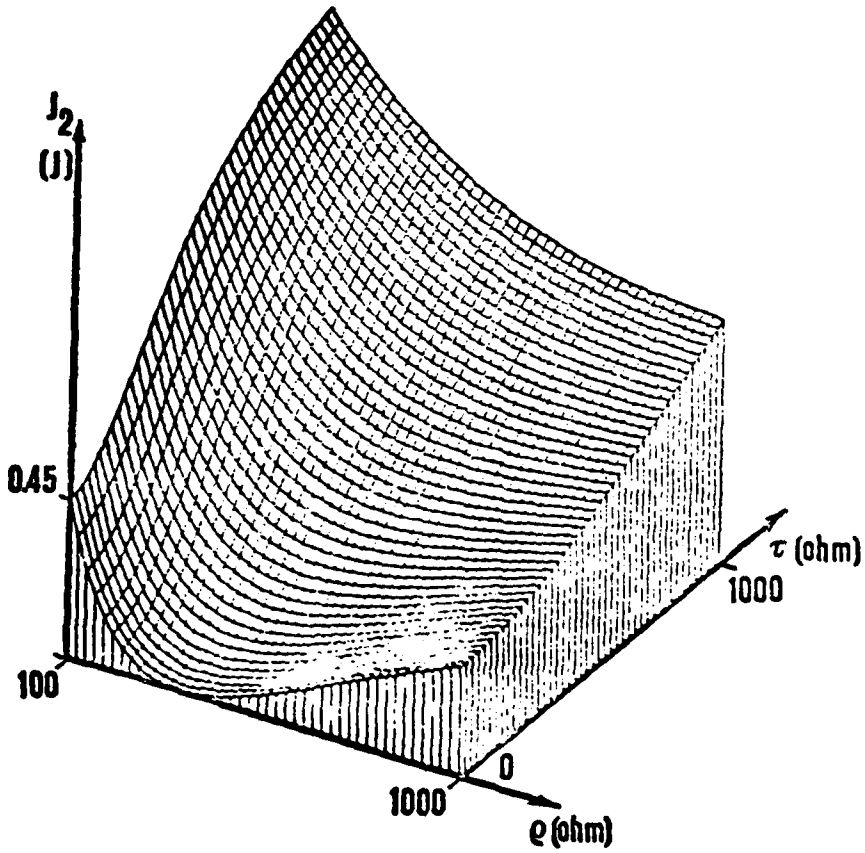

Figure 6. Time averaged electromagnetic energy in a volume, J_2. λ = 1m, d = 100m; $200 \leq r \leq 201$m; $0 \leq \theta \leq 0.5$ rad; $0 \leq \varphi \leq 0.5$ rad; $p = (1,0,0)$ Vs; $100 \leq \rho \leq 1000$ ohm; $0 \leq \tau \leq 1000$ ohm; (ρ,τ) domain divided into a 22×22 net. Minimum plotted value $J_{2min} = 0.008$ J at $z = (360 + i0)$ ohm. Maximum plotted value $J_{2max} = 0.8$ J at $z = (100 + i1000)$ ohm.

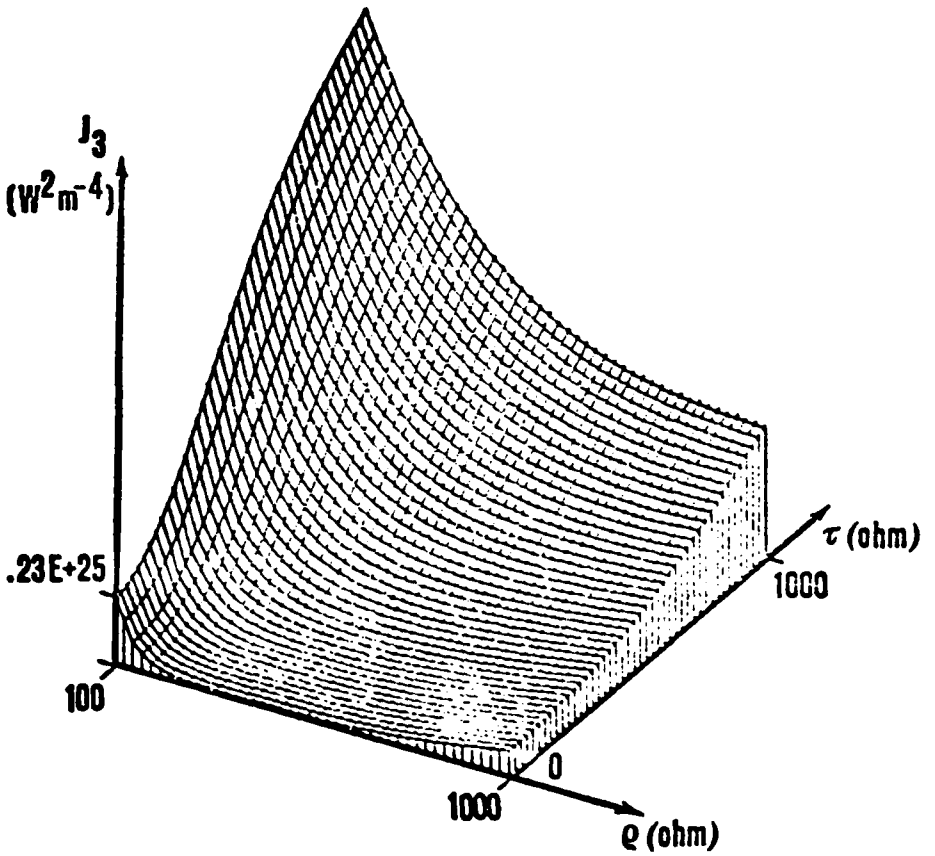

Figure 7. Time averaged squared modulus of Poynting vector at a point, J_3. λ,d as above; r = 200m; $\theta = \varphi = 0$ (source point); p as above; $(\rho;\tau)$ range of values and domain discretization as above. Minimum plotted value $J_{3min} \leq$ .63E + 22 W^2/m^4 at $\rho = 360 \pm 20$, $\tau = 0$ ohm. Maximum plotted value J_{3max} = .64E + 25 W^2/m^4 at z = 100 + i1000 ohm.

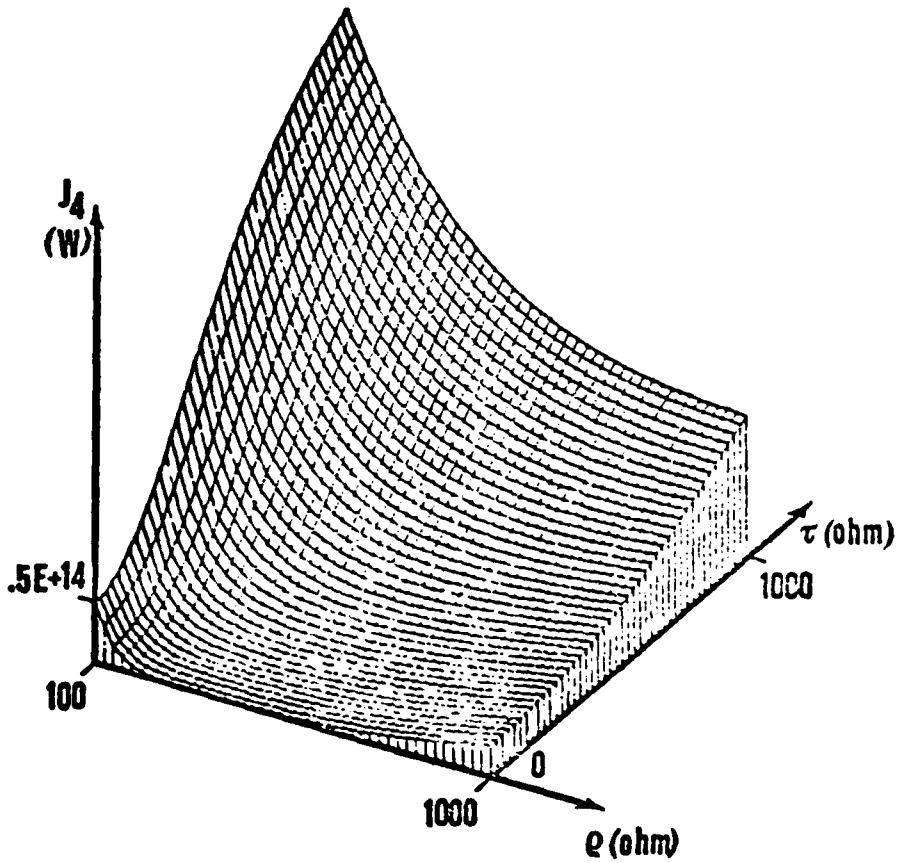

Figure 8. Time averaged flux of Re(S) through a surface, J_4. λ,d as above; r = 200m; $0 \leq \theta \leq 0.5$ rad; $0 \leq \varphi \leq 0.5$ rad; p as above; (ρ,τ) range of values and domain discretization as above. Minimum plotted value $J_{4min} < .7E + 11W$ at $z = 360 + i0$ ohm. Maximum plotted value $J_{4max} = .7E + 14W$ at $z = 100 + i1000$ ohm.

Table III. Minimization of J_1: optimal values of $\hat{\rho}$ vs. θ

λ = 1m; d = 100m; p = (1,0,0) Vs; φ = 0 rad

Re $\hat{z}$:= $\hat{\rho}$ in units of $\sqrt{\mu_0/\epsilon_0}$.

unconstrained: Re z and Im z independent; constrained: Re z = Im z

θ (rad)	r = 200m		r = 400m	
	unconstr.	constrained	unconstr.	constrained
0	1.0000	0.70708	1.0000	0.70708
	(source point)			
0.25	0.96891	0.68509	0.96891	0.68509
0.50	0.87758	0.62048	0.87758	0.62048
0.75	0.73169	0.51734	0.73169	0.51731
1.00	0.54030	0.38196	0.54030	0.38199
1.30	n.a.	n.a.	0.26750	0.18906

Table IV. Minimization of J_1 at source for different values of d

λ = 1m; r = 2d; θ = φ = 0; p = (1,0,0) Vs

computed optimal values ρ^k,τ^k are given in units of $\sqrt{\mu_0/\epsilon_0}$

	unconstrained					constrained			
	z^0 = (.265; 0,0)					z^0 = (.265E - 2; 0.0)			
d (m)	J_1^0 (J/m^3)	ρ^k (n.u.)	τ^k (n.u.)	J_1^k (J/m^3)	last it.(k)	J_1^0 (J/m^3)	$\rho^k = \tau^k$ (n.u.)	J_1^k (J/m^3)	last it.(k)
100	.26E + 3	1.0000	-.2E - 13	.71E - 27	40	.2E + 3	.70708	.34E + 2	13
200	.66E + 2	1.0000	-.8E - 13	.29E - 26	37	.19E + 3	.70708	.34E + 2	13
400	.16E + 2	1.0000	-.3E - 12	.11E - 25	34	.48E + 2	.70708	.84E + 1	15
800	.41E + 1	1.0000	-.1E - 11	.60E - 25	31	.12E + 2	.70715	.21E + 1	14

The typical CPU time required by a 30 iteration run is 0.25 s. The minimization of J_3 is carried out in a similar way and requires comparable CPU times. Some results are shown by Table V. Given e.g. z^0 = 1000 ohm, the convergence speed of $\{z^k\}$ is slightly higher in the "unconstrained" case and lower in the "constrained" one. The values of $\hat{z}$ computed by "constrained" minimization of J_1 and J_3 agree to within 3 decimal places (compare line 1, column 8 of Tables IV and V), which is an accuracy test for the computer code and its implementation.

J_2 and J_4 are dealt with by the same procedure, although for sake of brevity the results are not presented.

Table V. Minimization of J_3 at source for different values of d

λ = 1m; r = 2d; $\theta = \varphi = 0$; $\underline{p}$ = (1,0,0) Vs

computed optimal values ρ^k, τ^k are given in units of $\sqrt{\mu_0/\epsilon_0}$

	unconstrained z^0 = (2.652; 0.0)					constrained z^0 = (.265E - 2; 0.0)			
d (m)	$\sqrt{J_3^0}$ (W/m^2)	ρ^k (n.u.)	τ^k (n.u.)	$\sqrt{J_3^k}$ (W/m^2)	last it.(k)	$\sqrt{J_3^0}$ (W/m^2)	$\theta^k = \tau^k$ (n.u.)	$\sqrt{J_3^k}$ (W/m^2)	last it.(k)
100	.49E + 11	1.000	.19E - 7	.29E - 1	20	.23E + 12	.70746	.40E + 11	50
200	.12E + 11	1.000	.16E - 7	.72E - 2	20	.59E + 11	.71075	.10E + 11	30
400	.31E + 10	1.000	.15E - 7	.18E - 2	20	.15E + 11	.71082	.25E + 09	30
800	.77E + 09	1.000	.14E - 7	.45E - 3	20	.36E + 10	.71085	.63E + 09	30

III.5.4. The attraction domain of the minimization algorithm

Although the condition number criterion (3.20) applies wherever $\lambda_L > 0$, the algorithm is shown to yield a convergent sequence even if the starting value is well outside the subdomain G of (3.19). Minimization of J_1 at source is successful in the domain:

$$10^{-4} \leq \rho^0 \leq 10^4 \text{ ohm} ,$$
$$0 \leq \rho^0 \leq 10^4 \text{ ohm} . \qquad (3.25)$$

This is due to the fast search rule (3.18), which however becomes less effective when $|t^k J_z^{k*}| << |z^k|$. This occurs when $J^k/|J_z^k| >> 1$, because the cost function is rather "flat" at points far away from a minimum.

ACKNOWLEDGEMENTS

G. Crosta thanks Prof. G. Degli Antoni (Milan, Italy) for encouragement, Prof. R. Kleinman (Newark, DE) for a fruitful discussion, Dr. A. Kostinsky (Chicago, IL) for some comments.

All authors finally thank the referee for his constructive criticism.

REFERENCES

[1] D. S. Jones, Variational Methods in Electromagnetic Theory, Oxford: Oxford Univ. Press (1977).

[2] R. E. Collin, Antennas and Wave Propagation, New York: McGraw-Hill (1985).

[3] R. K. Luneburg, Mathematical theory of optics, Brown University lecture notes, Providence, R.I. (1944).

[4] J. B. Keller, "Geometrical theory of diffraction", J. Optical Soc. Amer., 52, 116-130 (1962).

[5] M. Klein and I. W. Kay, Electromagnetic Theory and Geometrical Optics), New York: J. Wiley & Sons (1964).

[6] T. B. A. Senior, "Diffraction by a semi-infinite metallic sheet", Proc. Royal Soc. London, A213, 436-458 (1952).

[7] G. Chen and T. J. Bridges, "Optimal boundary impedance for the minimization of reflection: (I) Asymptotic solutions by the geometrical optics method", Optimal Control, 6, 141-149 (1985).

[8] J. D. Jackson, Classical Electrodynamics, New York: J. Wiley & Sons (1969).

[9] J. B. Keller, R. M. Lewis, and B. D. Seckler, "Asymptotic solution to some diffraction problems", Comm. Pure and Appl. Math., 9, 207-265 (1956).

[10] G. Crosta, "On approximations of Helmholtz equation in the halfspace: Their relevance to inverse diffraction", Wave Motion, 6, 237-245 (1984).

[11] G. D. Malyughinetz, "Das Sommerfeld'sche Integral und die Lösung von Beugungsaufgaben in Winkelgebieten", Annalen d. Phys., 7. Folge, Bd. 6, 107-112 (1960).

[12] F. Giannessi, Metodi matematici della programmazione: problemi lineari e non lineari, Bologna: Pitagora (1982).

[13] B. Pchenitchny and Y. Daniline, Méthodes numériques dans les problèmes de extrémum, Ed. Mir, Moscow (1977).

[14] K. Zakrzewska, J. Dudek, and N. Nazarewicz, "A numerical calculation of multidimentional integrals", Computer Physics Comm., 14, 299-399 (1978).

[15] C. Lemarechal, "Methodes numeriques d'optimisation", Cahiers di Mathematiques de la Decision; Paris: Universite de Paris IX-Dauphine (1984).

TJB:GC:GC:scr

SECURITY CLASSIFICATION OF THIS PAGE (When Data Entered)

REPORT DOCUMENTATION PAGE

READ INSTRUCTIONS BEFORE COMPLETING FORM

1. REPORT NUMBER: 2942	2. GOVT ACCESSION NO.: AD-A172 585
3. RECIPIENT'S CATALOG NUMBER:	
4. TITLE (and Subtitle): MINIMIZING THE REFLECTION OF ELECTROMAGNETIC WAVES BY SURFACE IMPEDANCE	5. TYPE OF REPORT & PERIOD COVERED: Summary Report - no specific reporting period
	6. PERFORMING ORG. REPORT NUMBER:
7. AUTHOR(s): T. J. Bridges, G. Chen and G. Crosta	8. CONTRACT OR GRANT NUMBER(s): DMS-8210950, Mod. 4; DAAG29-80-C-0041; MCS78-22830 & DMS84-01297
9. PERFORMING ORGANIZATION NAME AND ADDRESS: Mathematics Research Center, University of Wisconsin, 610 Walnut Street, Madison, Wisconsin 53705	10. PROGRAM ELEMENT, PROJECT, TASK AREA & WORK UNIT NUMBERS: Work Unit Number 2 - Physical Mathematics
11. CONTROLLING OFFICE NAME AND ADDRESS: See Item 18 below.	12. REPORT DATE: July 1986
	13. NUMBER OF PAGES: 32
14. MONITORING AGENCY NAME & ADDRESS(if different from Controlling Office):	15. SECURITY CLASS. (of this report): UNCLASSIFIED
	15a. DECLASSIFICATION/DOWNGRADING SCHEDULE:

16. DISTRIBUTION STATEMENT (of this Report)

Approved for public release; distribution unlimited.

17. DISTRIBUTION STATEMENT (of the abstract entered in Block 20, if different from Report)

18. SUPPLEMENTARY NOTES

U. S. Army Research Office
P. O. Box 12211
Research Triangle Park
North Carolina 27709

National Science Foundation
Washington, DC 20550

19. KEY WORDS (Continue on reverse side if necessary and identify by block number)

electromagnetic waves
geometrical optics
control theory
minimizing reflection

20. ABSTRACT (Continue on reverse side if necessary and identify by block number)

In an empty halfspace a point rource emits electromagnetic waves of fixed frequency and arbitrary polarization. The fields reflected by an imperfectly conducting plane, characterized by a constant, isotropic surface impedance, are determined by means of the geometrical optics approximation. An optimization method is used to compute the surface impedance, which minimizes a given function of the e.m. fields (e.g. the average energy density) at a given observation point. The properties of the functions to be minimized are studied and a set of numerical results is presented and discussed.

DD FORM 1 JAN 73 1473 EDITION OF 1 NOV 65 IS OBSOLETE

UNCLASSIFIED

SECURITY CLASSIFICATION OF THIS PAGE (When Data Entered)

END

11-86

DTIC